

High-Resolution FTIR, Microwave, and Ab Initio Investigations of CH₂⁷⁹BrF: Ground, $\nu_5 = 1$, and $\nu_6 = 1, 2$ State Constants

Agostino Baldacci, Paolo Stoppa,* Andrea Pietropoli Charmet, and Santi Giorgianni

Dipartimento di Chimica Fisica, Università Ca' Foscari di Venezia, Calle Larga S. Marta 2137, I-30123, Venezia, Italy

Gabriele Cazzoli and Cristina Puzzarini*

Dipartimento di Chimica "G. Ciamician", Università di Bologna, Via Selmi 2, I-40126 Bologna, Italy

René Wugt Larsen†

Department of Chemistry, University of Copenhagen, Universitetsparken 5, DK-2100 Copenhagen, Denmark

Received: March 20, 2007; In Final Form: May 17, 2007

A spectroscopic study of CH₂⁷⁹BrF in the infrared and microwave regions has been carried out. The rovibrational spectrum of the ν_5 fundamental interacting with $2\nu_6$ has been investigated by high-resolution FTIR spectroscopy. Owing to the weakness of the $2\nu_6$ band, the $\nu_6 = 2$ state constants have been derived from $\nu_6 = 1$. For this reason, the rotational spectra of the ground and $\nu_6 = 1$ states have been observed by means of microwave spectroscopy. Highly accurate ab initio computations have also been performed at the CCSD(T) level of theory in order to support the experimental investigation. As far as the ν_5 band is concerned, the analysis of the rovibrational structure led to the identification of more than 3000 transitions, allowing the determination of a set of spectroscopic parameters up to sextic distortion terms and pointing out first-order *c*-type Coriolis interaction with the $\nu_6 = 2$ state. With regard to the pure rotational spectra measurements, the assignment of several $\Delta J = 0, +1$ transitions allowed the determination of the rotational, all the quartic, and most of the sextic centrifugal distortion constants, as well as the full bromine quadrupole coupling tensor for both the ground and $\nu_6 = 1$ states.

1. Introduction

The key to a thorough understanding of the chemical and physical properties of molecules is provided by their geometric structure. As far as experimental determination is concerned, rotational and rovibrational spectroscopy provides one of the most widely applicable and accurate methods.^{1,2} However, this requires the investigation of a sufficient number of isotopologues. In this view, the present study on bromofluoromethane is part of a wider project intended to fully characterize its different isotopic species in order to determine its molecular and structural properties.

Furthermore, during the past decades, halogen-containing molecules have attracted a great deal of attention because of their alarming connection with stratospheric ozone depletion and global warming.^{3–5} However, reliable experimental data for many halocarbons are still unavailable, especially for those containing bromine. On this topic, bromofluoromethane can potentially contribute to the destruction of stratospheric ozone since its ozone depletion potential (ODP) is 0.73 with respect to CFC-11.⁶ Although no information on environmental relevance is reported for this molecule, it could play a role in the chemical dynamics of atmospheric halogenated compounds. Generally, the determination of the atmospheric concentration

as well as the monitoring of the temporal trend is based on the solar infrared (IR) spectrum; in order to profit from the sensitivity of the spectroscopic techniques, one needs a satisfactory quantum assignment and accurate spectroscopic parameters.

High-resolution infrared spectra of this compound reveal a very dense rotational structure due to the absorption derived from main and hot bands of the bromine isotopologues in the natural sample (50.7/49.3 of ^{79/81}Br). The employment of synthesized isotopically enriched samples still leaves the spectrum congested; indeed the lowest vibrational state $\nu_6 = 1$ (311 cm⁻¹) generates rather strong hot bands, since the Boltzmann population at room temperature is about 23% with respect to the ground state.

An extensive low-resolution infrared study of this compound has been carried out, and results concerning fundamentals, overtones, combination bands, and hot bands have been reported.⁷ The high-resolution infrared spectrum of the synthesized enriched ⁷⁹Br sample has been investigated with a tunable diode laser in the ν_3 ⁸ and ν_4 ⁹ fundamental regions. The ground state rotational constants alone were determined many years ago from the microwave spectrum,¹⁰ whereas a more complete set also including all the quartic and a few sextic centrifugal distortion coefficients was reported not long ago by means of infrared combination differences from the ν_4 fundamental.⁹ Very recently, the ground state dipole moment of CH₂⁷⁹BrF was evaluated using microwave Stark spectroscopy.¹¹

The present work deals with a combined high-resolution infrared and microwave study on the two lowest lying funda-

* Corresponding authors. E-mail: stoppa@unive.it (P.S.); cristina.puzzarini@unibo.it (C.P.).

† Present address: Institut für Physikalische Chemie, Universität Göttingen, Tammanstr. 6, D-37077 Göttingen, Germany.

mentals (ν_5 , ν_6) and the ground state of CH₂⁷⁹BrF in conjunction with highly accurate ab initio computations. More precisely, theoretical values for the spectroscopic parameters have been used to guide the investigation as well as to confirm the corresponding interpretation of the spectra. The analysis of the ν_5 fundamental, located at 650.5 cm⁻¹, led to the identification of some irregularities in the spectrum. The observed perturbation effects allowed establishment of the presence of first-order *c*-type Coriolis resonance between $\nu_5 = 1$ and $\nu_6 = 2$ vibrational states, although the spectrum does not show any feature of the $2\nu_6$ overtone. In order to account for the interstate Coriolis interaction, it has been found necessary to employ the overtone rotational parameters, which could be approximately obtained from the ν_6 ones. The $\nu_6 = 1$ state constants have been determined in parallel with those of the ground state from microwave investigation. Furthermore, it is worth noting that the determination of the ν_5 and ν_6 parameters should be of great help for the study of the $\nu_5 + \nu_6$ combination which is expected to occur along with the ν_9 fundamental in the atmospheric window near 950 cm⁻¹.

2. Experimental and Computational Details

The enriched sample of CH₂⁷⁹BrF was prepared according to the procedure already described in a previous work (see ref 7 for all details). The percentage of the ⁷⁹Br in the sample was limited by the stated 90% form of NH₄⁷⁹Br (Sigma-Aldrich 99%) used as a precursor.

2.1. Microwave Measurements. Two spectrometers have been employed in the present measurements of the pure rotational spectrum. A centimeter-wave spectrometer, equipped with a conventional P band waveguide Stark cell 1.5 m long, has been used for the measurements in the 20–36 GHz frequency range, whereas a millimeter-wave spectrometer, equipped with a free-space cell, i.e., a glass tube, 3 m long and 5 cm in diameter, has been used for those in the 80–328 GHz frequency range. In the first case, the microwave source has been obtained by doubling the output of a computer-controlled frequency synthesizer (Model HP 8276A; 2–18 GHz), while the millimeter- and submillimeter-wave sources are either frequency multipliers driven by Gunn diode oscillators or Gunn diodes themselves. In all cases the microwave sources are phase-locked to a rubidium frequency standard. As far as detectors (whose output signal is processed by means of a lock-in amplifier) are concerned, an HP Schottky diode detector has been used in the centimeter- and millimeter-wave regions, whereas a liquid helium cooled InSb detector has been employed in the submillimeter-wave one. A detailed description of the centimeter- and millimeter-wave spectrometers can be found in refs 12 and 13, respectively.

The frequency modulation technique has been employed throughout, and second harmonic detections have been performed as the lock-in amplifier has been tuned at twice the modulation frequency (i.e., the second derivative of the spectra has been recorded). Computer-controlled data acquisition has been used: the driving of the spectrometer and the data processing have been carried out by means of homemade software. For each recorded spectrum, two frequency scans have been performed (forward and backward) and the number of points has been set according to the requirement. The frequency step and time constant employed were in the range 10–20 kHz and 10–30 ms, respectively.

The measurements have been carried out at room temperature employing pressures between 0.1 and 0.7 Pa. The modulation depth has been varied in the range 50–400 kHz according to

the gas pressure, whereas the modulation frequency has been kept fixed at 16.66 kHz. Even if the rotational spectrum of the ν_6 state is about 5 times weaker than that of the vibrational ground state, a good signal-to-noise ratio has been obtained, allowing an accuracy of ± 20 kHz in the retrieved frequency values as for the ground state itself.

2.2. Infrared Measurements. The infrared gas-phase-absorption spectrum has been recorded at 298 K using the Bruker IFS 120 HR Fourier transform spectrometer located at the H. C. Ørsted Institute, University of Copenhagen. The spectrometer uses a global broad-band IR source, a Ge on KBr beamsplitter, and a liquid nitrogen cooled HgCdTe (MCT) detector. The synthesized sample has been transferred to a 15 cm long White-type absorption cell equipped with KBr windows via a clean Pyrex glass/PTFE gas-handling system; a total optical path length of 240 cm has been employed with a sample pressure of 40 Pa.

Appropriate optical and electronic filters have been selected to eliminate aliasing and to reduce the photonic noise level and detector nonlinearity effects within the sampling fold points of 550 and 1400 cm⁻¹. The sample interferograms have been recorded with a spectral resolution of 0.0030 cm⁻¹ and transformed using Mertz phase correction, boxcar apodization, and a zero-filling factor of 2. The background interferogram of the evacuated absorption cell has been recorded with a resolution of 0.048 cm⁻¹, and then transferred and interpolated onto a wavenumber grid matching that of the sample spectrum using a zero-filling factor of 32. This background spectrum has been found sufficient to cancel out the most dominating interference fringes caused by the windows in the optical beam.

The absolute wavenumber scale of the resulting spectra has been calibrated against observed H₂¹⁶O absorption lines.¹⁴ The line positions have been fitted using the peak-finding function of Microcal ORIGIN 7.0. The precision of the observed line positions is estimated to be ± 0.0015 cm⁻¹.

2.3. Theoretical Prediction of the Rotational and Rovibrational Spectra. High-level quantum chemical calculations have been used to support the detection and the spectral assignment of bromofluoromethane, especially for vibrational excited states. To this purpose, accurate predictions of the relevant spectroscopic parameters and in particular of the rotational constants were needed. The coupled-cluster (CC) theory within the singles and doubles (CCSD) approximation augmented by a perturbative treatment of triple excitations (CCSD(T))¹⁵ has been employed throughout. This method has been chosen as it has been proven to give highly accurate results (see for instance refs 16–19). On the whole, the methodology described in the following is well-known to provide very reliable values (see, for example, refs 19–21).

An estimate of the equilibrium structure has been derived as described in ref 11. Briefly, the “best” structural parameters have been obtained by using a quintuple-zeta basis set and by accounting for the effect of additional diffuse functions as well as core correlation corrections. Scalar relativistic effects on Br have been treated by means of small core pseudopotentials. Then, this equilibrium geometry¹¹ has been employed for deriving the equilibrium rotational constants A_e , B_e , and C_e of the CH₂⁷⁹BrF isotopologue.

To get a prediction of the rotational constants for the vibrational ground and excited states of interest, the equilibrium rotational constants have been adequately corrected for vibrational effects:

$$B_v^i = B_e^i - \sum_r \alpha_r^i \left(\nu_r + \frac{1}{2} \right) \quad (1)$$

where the sum runs over all normal modes r , and α_r^i are the vibration–rotation interaction constants corresponding to the r th vibrational mode and the i th inertial axis. The anharmonic force field required for the theoretical determination of the α_r^i 's has been evaluated using a development version of the ACES II program package.²² The CCSD(T) level of theory has been employed in conjunction with the cc-pVTZ basis²³ in the frozen core approximation. The harmonic part has been obtained using analytic second derivatives of the energy,²⁴ and the corresponding cubic force field has been determined in a normal-coordinate representation via numerical differentiation of the analytically evaluated force constants as described in refs 25 and 26. Then, the cubic force field has been used to compute spectroscopic parameters using the usual second-order perturbation treatment of the rovibrational problem.²⁷

For the actual prediction of the spectrum of each vibrational state, in addition to the corresponding rotational constants, we have also employed the equilibrium quartic centrifugal distortion constants (obtained as a byproduct in the calculation of the harmonic force field) and the computed bromine quadrupole coupling tensor (obtained at the CCSD(T)/cc-pCVQZ level of theory, correlating all electrons) of the ground state. It must be noted that we decided to compute the quadrupole coupling tensor because old and not particularly accurate data (preliminary data with uncertainties of 2 MHz) were previously available in the literature.¹⁰ In addition, only the diagonal terms were known, while for such a Br-containing compound second-order effects are expected. To get very reliable results, the scalar relativistic effects, estimated at the multireference configuration interaction (MRCI) level of theory using the Douglas–Kroll–Hess Hamiltonian (MRCI/cc-pVTZ_DK),^{28,29} have been taken into account by making use of the additivity assumption.

3. Results and Discussion

As mentioned earlier, this work is a combined investigation of the ν_5 infrared band of CH₂⁷⁹BrF and of the microwave spectrum of the ground and $\nu_6 = 1$ states supported by ab initio calculations. The determination of the ν_6 constants was necessary to obtain the parameters of the $2\nu_6$ overtone which resulted to be the perturber of ν_5 .

3.1. The Ground and $\nu_6 = 1$ States. According to dipole moment measurements,¹¹ bromofluoromethane is expected to present strong b -type ($\mu_b = 1.704(26)$ D) and quite weak a -type ($\mu_a = 0.3466(11)$ D) spectra. In the present investigation rotational transitions with J ranging from 0 to 77 have been observed for both the ground and $\nu_6 = 1$ states. More precisely, mostly $\Delta J = 0$, $\Delta K_a = +1$, $\Delta K_c = -1$ (b -type) transitions have been recorded and assigned. In addition, strong $\Delta J = +1$, $\Delta K_a = +1$, $\Delta K_c = +1$ (b -type) and weaker $\Delta J = +1$, $\Delta K_a = 0$, $\Delta K_c = +1$ (a -type) transitions have also been recorded, where the latest ones have been observed in order to improve the determination of the rotational constants.

Prediction and simulation of the CH₂⁷⁹BrF rotational spectrum in its vibrational ground state have been performed by making use of theoretical data as well as experimental information available in the literature.^{9,10} Thanks to the good predictions available, even if the rotational spectrum is greatly complicated by the fine structure due to the bromine quadrupolar nucleus, the assignment has been successfully carried out. In Figure 1 an example of the spectrum at ~ 102 GHz is given. In particular,

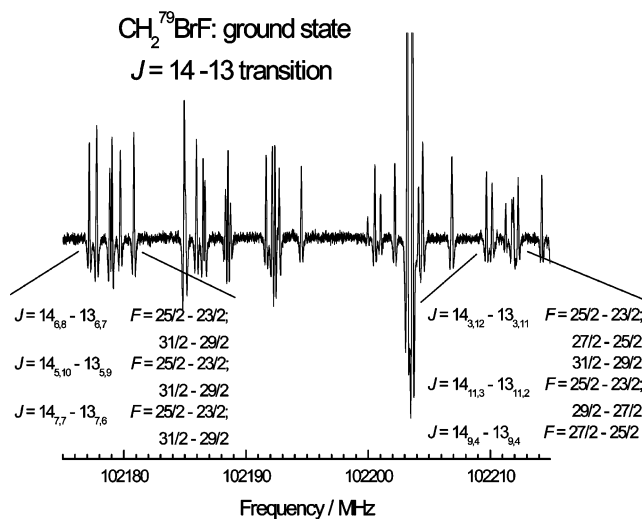


Figure 1. Rotational spectrum of the ground state of CH₂⁷⁹BrF. A portion of the $J = 14 \leftarrow 13$ transition (~ 102 GHz) shows the overcrowding of the fine structure due to the bromine quadrupole coupling. For clarity reasons, only a few quantum numbers are reported.

a portion of the $J = 14 \leftarrow 13$ transition (a -type lines) shows the overcrowding of the fine structure.

Since no experimental data were available in the literature concerning the rotational parameters of $\nu_6 = 1$, it was fundamental to get a theoretical prediction of the rotational spectrum. This has been obtained as briefly mentioned in the computational details section. It is also interesting to notice that this spectrum presents characteristic $\Delta J = 0$, $\Delta K_a = +1$, $\Delta K_c = -1$ bands, and we concentrated our attention on them. The spectral assignment has been carried out iteratively by comparing the graphical representation of the predicted spectrum to the observed one. The most characteristic features (due to the bromine quadrupole coupling and/or to the K doublets splitting) were assigned first, and this allowed improvement of the rotational and centrifugal distortion constants. By using improved parameters, new predictions have been made which allowed further assignments. This iterative procedure has been repeated until the full assignment has been achieved. An example of the comparison between calculated and observed spectra is provided by Figure 2, where a portion of the band head at 327 GHz ($\Delta J = 0$, $\Delta K_a = +1$, $\Delta K_c = -1$ band with $K_a = 4$) is depicted.

A total of 534 and 344 distinct rotational frequency lines have been recorded and assigned for the ground and $\nu_6 = 1$ states, respectively. To determine the rotational parameters, the transition frequencies have been included in a least-squares fit in which each line has been weighted proportionally to the inverse square of its experimental uncertainty. The fit has been carried out using Watson's A-reduced Hamiltonian in the I' representation³⁰ with Pickett's SPCAT/SPFIT program,³¹ and the results are summarized in Table 1, where they are compared with the previous data available in the literature. It must be noted that for both states the assigned lines allowed us to determine, in addition to the rotational constants, all the quartic and most of the sextic centrifugal distortion constants. As far as the bromine quadrupole coupling tensor is concerned, it should be stressed that, as expected, second-order effects have been observed, and the full tensor (even the off-diagonal term χ_{ab}) along with the J -dependence of the large diagonal term, χ_{aa}^J , has been obtained for the first time.

From Table 1 it is clear that the obtained results are in good agreement with those available in the literature. Nevertheless,

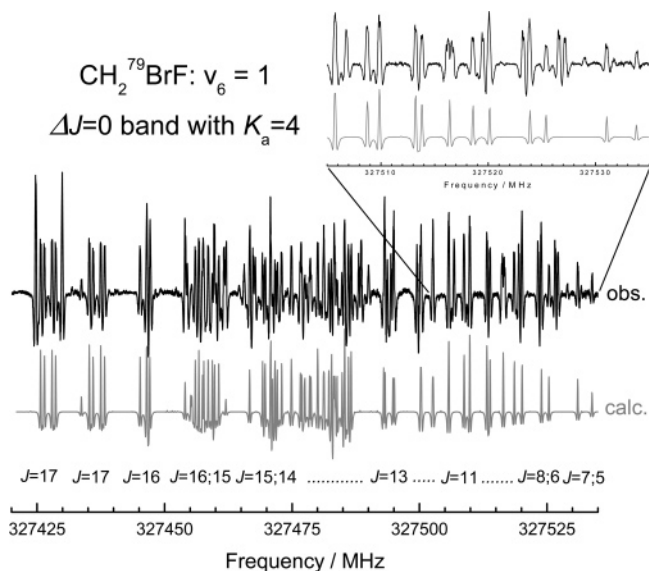


Figure 2. Rotational spectrum of the $\nu_6 = 1$ state of CH₂⁷⁹BrF. Upper trace: observed spectrum of a portion of the $\Delta J = 0$, $\Delta K_a = +1$, $\Delta K_c = -1$ band with $K_a = 4$ (~ 327 GHz). Lower trace: calculated spectrum. Inset: a detailed portion of the band head. For clarity reasons, only a few quantum numbers are reported.

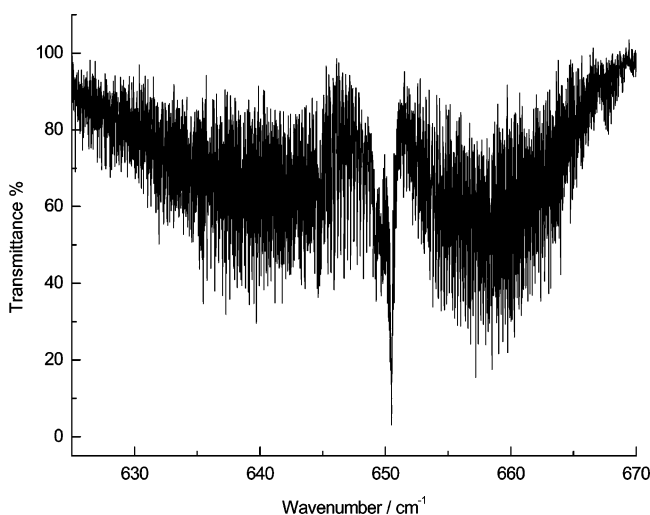


Figure 3. Survey spectrum of the ν_5 band of CH₂⁷⁹BrF ($T = 298$ K, $P = 40$ Pa, 240 cm optical path length).

the present measurements allowed us to largely improve all the parameters and to determine some new centrifugal distortion constants. With regard to ν_6 , one may notice that the spectroscopic parameters have been derived with an accuracy comparable to that reached for the ground state.

3.2. The ν_5 Fundamental and the $\nu_5 = 1/\nu_6 = 2$ States Interaction. Bromofluoromethane has one plane of symmetry (the F–C–Br plane) and belongs to the C_s point group. The nine fundamental vibrations and their up-to-date band origins are reported in ref 8. The molecule is a near-prolate asymmetric top ($\kappa = -0.986$), and the rotational structure of the bands approximates that of symmetric rotors. The ν_5 mode belonging to the A' symmetry species should give rise to an a - b -hybrid band. The observed fine structure is that of the a -type component, and this is in agreement with the C–Br stretching vibration involving distortion of the molecule mainly in the direction of the a inertial axis. Therefore, the applied selection rules for the strongest transitions are $\Delta J = 0, \pm 1$, $\Delta K_a = 0$ and

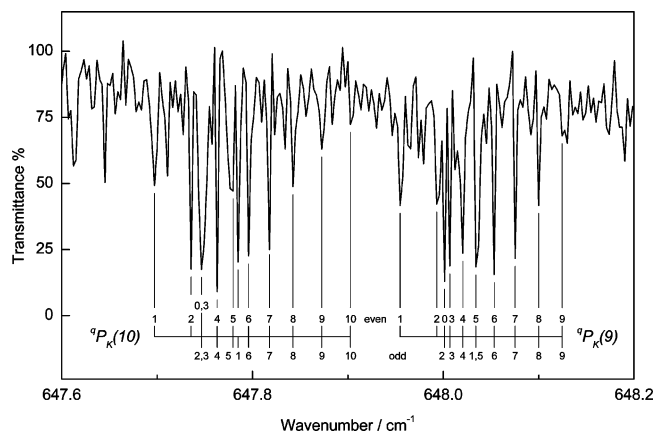


Figure 4. Section of the P-branch spectrum of CH₂⁷⁹BrF ν_5 band showing the structure of the ${}^9P_{K_a}(J)$ multiplets with $K_a = 9, 10$ ($T = 298$ K, $P = 40$ Pa, 240 cm optical path length). The even and odd labels correspond to $K_a'' + K_c'' = J''$ and $K_a'' + K_c'' = J'' + 1$, respectively.

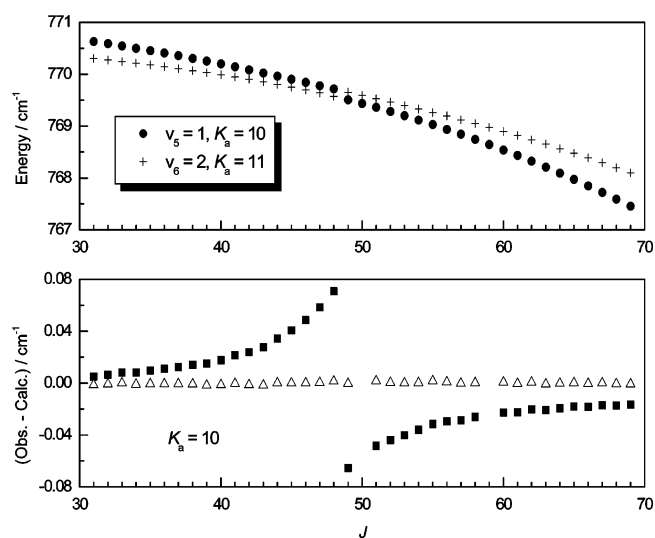


Figure 5. Observed crossing and calculated residuals for the $K_a = 10$ perturbed level of CH₂⁷⁹BrF $\nu_5 = 1$ state. Upper: rovibrational energy levels for $K_a = 10$ of $\nu_5 = 1$ (circles) and $K_a = 11$ of $\nu_6 = 2$ states (crosses). The energies have been calculated from the constants given in Table 2, reduced by $(1/2)(B_0 + C_0)J(J + 1)$. Lower: deviations of the $K_a = 10$ transitions of the ν_5 band before (squares) and after (open triangles) the treatment of Coriolis perturbation.

$\Delta K_c = \pm 1$. The high-resolution survey spectrum of the ν_5 band is illustrated in Figure 3, which shows a noticeable line density even in the P- and R-branches. The dominant Q-branch is unstructured, while the 9 P- and 9 R-subbranches for low J values clearly emerge as clusters through the large number of weaker lines. Figure 4 illustrates the K_a sequence for two J -multiplets of ν_5 in the P-branch. Asymmetry splitting is here evident for the $K_a = 1$ and 2 transitions.

The process of assignment initiated with spectra simulations near the band center assuming the ground state parameters of the present work and the predicted rotational constants for the upper level obtained from ab initio calculations. The consistency of assignment has been checked by ground state combinations differences. The process of line identifications has been assisted by correlation diagrams which combine the P-, Q-, and R-transitions reaching the same upper level, according to the Nakagawa and Overend procedure.³² The assignment within the K_a subbands was not difficult in most cases; the asymmetry splitting has been observed up to $K_a = 6$ for $J'' \geq 68$ and the

TABLE 1: Spectroscopic Parameters for the Ground and $\nu_6 = 1$ States of $\text{CH}_2^{79}\text{BrF}^a$

parameters	ground state			$\nu_6 = 1$ state this work
	ref 10	ref 9	this work	
A (MHz)	39 852.5	39 852.671 (30)	39 852.971 18 (62)	40 053.302 36 (94)
B (MHz)	3772.9	3772.924 (12)	3772.957 168 (69)	3767.944 04 (10)
C (MHz)	3523.9	3524.060 (12)	3523.953868 (71)	3517.271 80 (10)
Δ_J (kHz)		1.77687 (90)	1.787928 (51)	1.7879 28 (56)
Δ_{JK} (kHz)		-24.544 (24)	-24.7916 (13)	-24.892 10 (99)
Δ_K (kHz)		535.64 (21)	538.660 (28)	556.223 (34)
δ_J (kHz)		0.17658 (60)	0.183517 (16)	0.184696 (19)
δ_K (kHz)		6.00 (60)	8.0991 (70)	8.7927 (83)
Φ_J (Hz)			0.0009003 (72)	0.0008624 (90)
Φ_{JK} (Hz)		0.0210 (30)	0.01077 (22)	0.01121 (22)
Φ_{KJ} (Hz)		-1.439 (30)	-1.939 (13)	-2.0116 (56)
Φ_K (Hz)		19.49 (30)	25.12 (57)	27.25 (34)
ϕ_J (Hz)			0.0002630 (29)	0.0002703 (33)
ϕ_{JK} (Hz)			0.0248 (14)	0.0246 (18)
χ_{aa} (MHz)	443.5 (20)		443.531 (24)	444.167 (39)
χ_{bb} (MHz)	-145.0 (20)		-144.980 (34)	-145.506 (42)
χ_{cc} (MHz)	-298.5 (20)		-298.551 (34)	-298.657 (42)
$ \chi_{ab} $ (MHz)			278.63 (54)	277.23 (43)
χ_{aa}^I (MHz)			-0.00839 (66)	-0.0072 (11)
σ (kHz)			22.8	23.9

^a Quoted uncertainties in parentheses are one standard deviation in units of the last significant digits.

TABLE 2: Spectroscopic Constants (cm^{-1}) for the Ground, $\nu_5 = 1$, and $\nu_6 = 2$ States of $\text{CH}_2^{79}\text{BrF}^a$

	ground state	$\nu_5 = 1$	$\nu_6 = 2$
ν_0		650.487 227 (105)	623.1736 (99)
A	1.329 352 027 (21)	1.330 376 2 (26)	1.342 716 685 ^b
B	0.125 852 30 44 (23)	0.125 201 132 (150)	0.126 464 (50)
C	0.117 546 448 4 (24)	0.116 860 568 (163)	0.115 985 (48)
$\Delta_J \times 10^7$	0.596 389 (17)	0.593 79 (38)	0.596 389 ^c
$\Delta_{JK} \times 10^6$	-0.826 959 (43)	-0.838 91 (127)	-0.826 959 ^c
$\Delta_K \times 10^4$	0.179 677 6 (93)	0.180 485 (147)	0.179 677 6 ^c
$\delta_J \times 10^8$	0.612 147 (53)	0.610 66 (82)	0.612 147 ^c
$\delta_K \times 10^6$	0.270 16 (23)	0.2704 (34)	0.270 16 ^c
$\Phi_J \times 10^{13}$	0.3003 (24)	0.302 (33)	0.3003 ^c
$\Phi_{JK} \times 10^{12}$	0.3592 (73)	0.474 (134)	0.3592 ^c
$\Phi_{KJ} \times 10^{10}$	-0.6468 (43)	-0.604 (34)	-0.6461 ^c
$\Phi_K \times 10^9$	0.838 (19)	0.908 (21)	0.838 ^c
$\phi_J \times 10^{14}$	0.8773 (97)	0.8773 ^c	0.8773 ^c
$\phi_{JK} \times 10^{12}$	0.827 (47)	0.827 ^c	0.827 ^c
$\xi_{5,66}^c \times 10^2$			0.3142 (29)
no. of data		3010	
J_{max}		95	
$K_{a,\text{max}}$		23	
$\sigma \times 10^3$			0.834

^a Quoted uncertainties in parentheses are one standard deviation in units of the last significant digits. ^b Fixed to the rotational constant obtained assuming that eq 1 applies. ^c Fixed to the ground state value.

largest splitting was reached for the $K_a = 3$ sublevel. Due to severe blending, also caused by hot bands and the absorptions of the ^{81}Br isotopologue still present in the sample, many assigned lines have been removed from the data set. The identified transitions could be fitted within the precision of the measurements to the Watson type Hamiltonian in the A -reduction and I' -representation³⁰ with the exclusion of the perturbed ones belonging to the $K_a = 10$ stack, which showed consistent displacements from the calculated values. The negative and positive residuals (observed - calculated values) of the transitions involving the upper sublevel $K_a = 10$ are reproduced in Figure 5, where the avoided crossing at $J = 48-49$ is shown. No other crossings have been observed in the analyzed region.

The ν_5 band is far from any other fundamental; hence, the perturber must be an overtone or a combination. Among them the only one close in energy is $2\nu_6$ (A'), expected to lie about 28 cm^{-1} below ν_5 . As is well-known, vibrational anharmonic ($|\Delta K_a| = 0, 2, \dots$) and c -type Coriolis ($|\Delta K_a| = 1, 3, \dots$)

resonances may occur between levels of the same symmetry species. Assuming for ν_5 and $2\nu_6$ the same rotational constants for the ground and excited states, calculations of the rovibrational energy levels in the prolate symmetric-top limit suggest that the interaction is through first-order c -type Coriolis resonance. Once more, it is worthwhile noting that direct transitions to the perturber $2\nu_6$ have not been observed. In the course of the interaction study the $\nu_5 = 1$ and $\nu_6 = 2$ states have been treated simultaneously using Pickett's SPCAT/SPFIT program³¹ with an effective two state rotational Hamiltonian matrix of the form

$$\begin{vmatrix} \mathbf{H}_r(5) & \mathbf{H}_c \\ \mathbf{H}_c & \mathbf{H}_r(66) \end{vmatrix} \quad (2)$$

where $\mathbf{H}_r(5)$ and $\mathbf{H}_r(66)$ represent the above-mentioned Watson's Hamiltonian for the $\nu_5 = 1$ and $\nu_6 = 2$ states, respectively, and \mathbf{H}_c is the Coriolis operator employed in the form

$$\mathbf{H}_c = i \xi_{5,66}^c \mathbf{P}_c \quad (3)$$

which gives rise to the following matrix elements:

$$\langle J, K | \mathbf{H}_c | J, K \pm 1 \rangle = \pm \frac{1}{2} \xi_{5,66}^c \sqrt{J(J+1) - K(K \pm 1)} \quad (4)$$

where $\xi_{5,66}^c = \xi_{5,66}^c C_e(\omega_5 + \omega_{66})/(\omega_5 \omega_{66})^{1/2}$.

In the fitting procedure, the ground state constants have been fixed at the values determined in the present study. As initial parameters for the $\nu_5 = 1$ state, the constants derived from the fit of the less perturbed assigned transitions have been used, whereas for $\nu_6 = 2$ state the band origin has been obtained from ref 7 using harmonic approximation and the rotational constants have been deduced from those of the $\nu_6 = 1$ state assuming that eq 1 applies. As far as the coupling parameter $\xi_{5,66}^c$ is concerned, an estimated value of 0.0028 cm⁻¹ has been derived using the maximum residual shown in Figure 5. Finally, the transition wavenumbers have been fitted by assuming uncertainties of 0.0015 cm⁻¹ for apparently single lines and 0.0030 cm⁻¹ for blended features.

Satisfactory results have been obtained by constraining for the $\nu_6 = 2$ state the rotational constant A to the value coming from the $\nu_6 = 1$ state (considering eq 1) and the centrifugal distortion terms to those of the ground state. The best results obtained from the model connecting the two interacting levels are reported in Table 2, which also includes, for comparison purposes, the ground state parameters in units of cm⁻¹. From this table one may notice that the ν_5 spectroscopic constants are well-defined and the values of the determined constants are close to those of the ground state. Concerning the $\nu_6 = 2$ state parameters, it should be emphasized that, on one hand, the rotational constant A has been kept constrained since it is strongly correlated with the band origin and, on the other hand, the other parameters are to be considered only effective since the B and C constants are also strongly correlated with each other. Nevertheless, the model employed allowed us to fit all the data within their experimental uncertainties and to determine the Coriolis coupling.

For the sake of completeness, it is worthwhile to point out that the Fermi interaction between ν_5 and $2\nu_6$ has also been considered, but no meaningful value for the $W_{5,66}$ constant could be achieved. Therefore, the resonance must be considered very weak, with this also being inferred from the absence of any spectral feature of $2\nu_6$ which, to some extent, should have been involved in a "borrowing intensity" process from ν_5 .

3.3. Comparison of Experimental and Computed Spectroscopic Parameters. The theoretical results, reported in Table 3, are compared with the available experimental data. From this table an overall good agreement is observed confirming the predictive capabilities of highly accurate ab initio computations, which, therefore, may be considered a useful support to the experimental investigation. On this topic, it should be noted that calculated values were checked by using the experimental values available in the literature prior to this work.⁷⁻¹⁰

Concerning the bromine quadrupole coupling constants, the deviations from experiment are well within 0.5% and the relativistic corrections are small but relevant, being about 1%. With respect to the other spectroscopic parameters, the ground state rotational constants agree with experiment within 0.1%, while the quartic centrifugal distortion constants present discrepancies on the order of 2–8%. Furthermore, the good agreement observed for the best estimated rotational constants of the $\nu_5 = 1$ and $\nu_6 = 1$ states (the discrepancies are better than 0.5%) underlines the accuracy achieved in the theoretical

TABLE 3: Theoretical Spectroscopic Parameters of CH₂⁷⁹BrF: Comparison with Experiment

parameters	theory ^a	experiment
ν_1 (cm ⁻¹)	2991.6	2992.6 ^b
ν_2 (cm ⁻¹)	1468.7	1465.4 ^b
ν_3 (cm ⁻¹)	1315.6	1314.1 ^b
ν_4 (cm ⁻¹)	1085.3	1068.1 ^b
ν_5 (cm ⁻¹)	644.3	650.6 ^b
ν_6 (cm ⁻¹)	310.6	311.0 ^b
ν_7 (cm ⁻¹)	3042.6	3047.2 ^b
ν_8 (cm ⁻¹)	1231.1	1226.7 ^b
ν_9 (cm ⁻¹)	934.3	935.2 ^b
	ground state	
A (MHz)	39 802.09	39 852.971 18 (62)
B (MHz)	3769.47	3772.957 168 (69)
C (MHz)	3525.61	3523.953 868 (71)
Δ_J (kHz)	1.70	1.787 928 (51)
Δ_{JK} (kHz)	-24.37	-24.7916 (13)
Δ_K (kHz)	541.10	538.660 (28)
δ_J (kHz)	0.17	0.183 517 (16)
δ_K (kHz)	7.43	8.0991 (70)
χ_{aa} (MHz)	442.85	443.531 (24)
χ_{bb} (MHz)	-145.82	-144.980 (34)
χ_{cc} (MHz)	-297.03	-298.551 (34)
$ \chi_{ab} $ (MHz)	277.50	278.63 (54)
	$\nu_6 = 1$	
A (MHz)	40 001.13	40 053.302 36 (94)
B (MHz)	3764.75	3767.944 04 (10)
C (MHz)	3519.26	3517.271 80 (10)
	$\nu_5 = 1$	
A (MHz)	39826.79	39883.675 (78)
B (MHz)	3750.17	3753.4355 (45)
C (MHz)	3505.45	3503.3917 (49)
	$\nu_6 = 2$	
A (MHz)	40 200.17	40 253.634 ^c
B (MHz)	3760.03	3791.3 (15) ^c
C (MHz)	3512.91	3477.1 (14) ^c
$\xi_{5,66}^c$ (cm ⁻¹)	0.003	0.0031 42 (29)
	$\nu_9 = 1$	
A (MHz)	39 711.30	
B (MHz)	3760.09	
C (MHz)	3514.97	
	$\nu_5 = 1, \nu_6 = 1$	
A (MHz)	40 025.83	
B (MHz)	3745.45	
C (MHz)	3499.10	

^a Fundamental frequencies from the anharmonic force field at the (fc)CCSD(T)/cc-pVTZ level. Rotational constants obtained by adding to the best estimated equilibrium rotational constants vibrational corrections at the (fc)CCSD(T)/cc-pVTZ level. Quartic centrifugal distortion constants ((fc)CCSD(T)/cc-pVTZ level) are equilibrium values. Nuclear quadrupole coupling constants at the (all) CCSD(T)/cc-pCVQZ level corrected for scalar relativistic effects (see text). ^b Reference 7. ^c A constant fixed assuming that eq 1 applies; B and C effective parameters. See text.

prediction of the vibration–rotation interaction constants. Finally, deviations ranging from 0.1% to 1.5% are noted for fundamental frequencies.

Since anharmonic force field computations have been carried out, the interaction between ν_5 and $2\nu_6$ can also be estimated. On the basis of the quadratic and cubic force constants at the CCSD(T)/cc-pVTZ level, weak Fermi ($W_{5,66} = -11.43$ cm⁻¹) and first-order c -type Coriolis ($\xi_{5,66}^c = 0.003$ cm⁻¹) interactions are predicted, with the latter being also experimentally confirmed. As far as the Fermi resonance is concerned, it is important to note that the value estimated for $W_{5,66}$ in conjunction with the frequency separation between ν_5 and $2\nu_6$ (~24

TABLE 4: Principal Quadrupole Tensor for ^{79}Br in $\text{CH}_2^{79}\text{BrF}$

parameters	theory	experiment
χ_{zz} (MHz)	553.04	554.52 (38)
χ_{xx} (MHz)	-256.01	-255.97 (38)
χ_{yy} (MHz)	-297.03	-298.551 (34)
η	0.074	0.076 79 (17)
θ_{za} (deg)	21.66	21.7188 (49)
$\angle(\text{CBr}.a)$ (deg)	21.13	
$\delta = \theta_{za} - \angle(\text{CBr}.a)$ (deg)	0.53	

cm^{-1}) would lead to a band origin shift lower than 1 cm^{-1} , explaining why there is no experimental evidence of this resonance.

Finally, since the $\nu_5 + \nu_6$ combination and the ν_9 fundamental may have some atmospheric relevance, the theoretical prediction of their rotational constants is also included in Table 3. On the basis of the results obtained for ν_5 and ν_6 , the accuracy of these values is expected to be on the order of 0.5%.

3.4. Quadrupole Coupling Tensor and Related Chemical Information. Determination of the full nuclear quadrupole tensor χ^I in inertial axes (Table 1) allows the derivation of the principal nuclear quadrupole tensor χ^P . This yields the orientation, at the quadrupolar nucleus, of the principal quadrupole axes relative to the principal inertial axes. Because of the C_s symmetry of the molecule, $\chi_{yy} \equiv \chi_{cc}$. Values of χ_{zz} , χ_{xx} , and the absolute value of θ_{za} have been derived from diagonalizing χ^I , where z is the axis in the direction of the largest magnitude of the field gradient, and θ_{za} is the angle between the a and z axes. Experimental and theoretical results are summarized in Table 4.

The knowledge of the principal nuclear quadrupole tensor provides the opportunity to assess the asymmetry of the field gradient at the Br nucleus, which is expressed by the asymmetry parameter η . Since the z -axis is usually taken along the bond axis of the quadrupolar nucleus considered, the standard quadrupole asymmetry parameter

$$\eta = \frac{\chi_{xx} - \chi_{yy}}{\chi_{zz}} \quad (5)$$

reflects, in the first instance, elliptical type distortion of electron density in a plane perpendicular to the bond axis. From Table 4 it is evident that the asymmetry parameter η is well reproduced by ab initio calculations: it differs from the experimental value by less than 4%. Nevertheless, the direction of the z -axis is usually not exactly collinear with the internuclear axis; thus another asymmetry parameter must be introduced. This is the δ angle, which is given by the difference between the rotation angle θ_{za} and the angle formed by the internuclear axis and the inertial a -axis. The theoretical δ value is reported in Table 4: it is worth mentioning that a very small angular deviation, 0.53° , has been found. Since no experimental structure is presently available, we are not able to provide the experimental value of the asymmetry parameter δ ; however, on the basis of the accuracy of the other computed parameters, we are confident that the ab initio value is reliable.

Using a simple model,^{1,33} based on an approximate method developed by Townes and Dailey,³⁴ the ionic and π contributions to the C-Br bond have been evaluated from the principal quadrupole coupling constants. The resulting π character is small, being about 3%. On the other hand, a relevant ionic contribution has been found, i.e., on the order of 35%.

4. Conclusions

In the present work a spectroscopic investigation of $\text{CH}_2^{79}\text{BrF}$ has been carried out: the rotational spectra of the ground and $\nu_6 = 1$ states have been observed by means of microwave spectroscopy, and the rovibrational spectrum of ν_5 perturbed by $2\nu_6$ has been investigated through high-resolution FTIR spectroscopy. Concerning the vibrational ground state, this study provides an improvement of the spectroscopic constants available in the literature and the determination of further sextic centrifugal distortion constants together with some new bromine quadrupole coupling terms. With respect to the vibrational excited states, a set of spectroscopic parameters up to sextic distortion terms have been accurately evaluated for the first time. Furthermore, first-order c -type Coriolis interaction between the $\nu_5 = 1$ and $\nu_6 = 2$ states has been assessed. The experimental study has been supported by quantum chemical calculations that played a relevant role in the spectra prediction as well as in the assignment procedure.

The measured transition frequencies of the vibrational states investigated, not reported in the paper, are available from the authors upon request.

Acknowledgment. This work has been supported by “PRIN 2005” funds (project “Trasferimenti di energia e di carica a livello molecolare”), by the University of Bologna (funds for selected research topics and RFO funds), and by the University of Venice (FRA funds). The authors thank Mr. A. Baldan (Dipartimento di Chimica Fisica, Università di Venezia) for preparing the isotopically enriched sample of $\text{CH}_2^{79}\text{BrF}$. C.P. gratefully thanks Prof. J. Gauss for providing the development version of the ACES2 program package. R.W.L. acknowledges a grant from the Danish Research Council.

References and Notes

- Gordy, W.; Cook, R. L. *Microwave molecular spectra*, 3rd ed.; Weissberger, A., Ed.; John Wiley & Sons: New York, 1984.
- Hollas, J. M. *High resolution spectroscopy*, 2nd ed.; John Wiley & Sons: New York, 1998.
- Atkinson, R. *Atmos. Environ.* **1990**, *24A*, 1–41.
- Atkinson, R.; Carter, W. P. L. *Chem. Rev.* **1984**, *84*, 437–470.
- Atkinson, R. *Chem. Rev.* **1986**, *86*, 69–201.
- World Meteorological Organization (WMO). *Scientific Assessment of Ozone Depletion: 2002*; Global Ozone, Research and Monitoring Project; Report 47; WMO: Geneva, 2003.
- Baldacci, A.; Baldan, A.; Gambi, A.; Stoppa, P. *J. Mol. Struct.* **2000**, *517–518*, 197–208.
- Baldacci, A.; Stoppa, P.; Pietropolli Charmet, A.; Giorgianni, S. *J. Mol. Spectrosc.* **2003**, *220*, 7–12.
- Baldacci, A.; Stoppa, P.; Gambi, A. *J. Mol. Spectrosc.* **2000**, *201*, 280–284.
- Curnuck, P. A.; Sheridan, J. *Nature* **1964**, *202*, 591–592.
- Cazzoli, G.; Puzzarini, C.; Baldacci, A.; Baldan, A. *J. Mol. Spectrosc.* **2007**, *241*, 112–115.
- Dore, L.; Cludi, L.; Mazzavillani, A.; Cazzoli, G.; Puzzarini, C. *Phys. Chem. Chem. Phys.* **1999**, *1*, 2275–2278.
- Cazzoli, G.; Dore, L. *J. Mol. Spectrosc.* **1990**, *143*, 231–236.
- Toth, R. A. *J. Opt. Soc. Am. B* **1991**, *8*, 2236–2255.
- Raghavachari, K.; Trucks, G. W.; Pople, J. A.; Head-Gordon, M. *Chem. Phys. Lett.* **1989**, *157*, 479–483.
- Helgaker, H.; Jørgensen, P.; Olsen, J. *Molecular Electronic-Structure Theory*; Wiley: Chichester, New York, 1999.
- Bak, K. L.; Gauss, J.; Jørgensen, P.; Olsen, J.; Helgaker, T.; Stanton, J. F. *J. Chem. Phys.* **2001**, *114*, 6548–6556.
- Coriani, S.; Marchesan, D.; Gauss, J.; Hättig, C.; Jørgensen, P.; Helgaker, T. *J. Chem. Phys.* **2005**, *123*, 184107-1–184107-12.
- Puzzarini, C.; Cazzoli, G.; Gambi, A.; Gauss, J. *J. Chem. Phys.* **2006**, *125*, 054307-1–054307-8.
- Cazzoli, G.; Puzzarini, C.; Gambi, A.; Gauss, J. *J. Chem. Phys.* **2006**, *125*, 054313-1–054313-8.
- Puzzarini, C. *J. Chem. Phys.* **2005**, *123*, 024313-1–024313-14.

(22) Stanton, J. F.; et al. *ACES II* (Mainz–Austin–Budapest version); a quantum-chemical program package for high-level calculations of energies and properties; see <http://www.aces2.de>.

(23) Dunning, T. H., Jr. *J. Chem. Phys.* **1989**, *90*, 1007–1023.

(24) Gauss, J.; Stanton, J. F. *Chem. Phys. Lett.* **1997**, *276*, 70–77.

(25) Stanton, J. F.; Lopreore, C. L.; Gauss, J. *J. Chem. Phys.* **1998**, *108*, 7190–7196.

(26) Stanton, J. F.; Gauss, J. *Int. Rev. Phys. Chem.* **2000**, *19*, 61–95.

(27) Mills, I. M. *Molecular Spectroscopy: Modern Research*; Narahari, R. K., Mathews, C. W., Eds.; Academic: New York, 1972.

(28) MOLPRO is a package of ab initio programs written by H.-J. Werner and P. J. Knowles, with contributions from Amos, R. D.; Bernhardsson, A.; Celani, P.; Cooper, D. L.; Deegan, M. J. O.; Dobbyn, A. J.; Eckert, F.; Hampel, C.; Hetzer, G.; Korona, T.; Lindh, R.; Lloyd, A.

W.; McNicholas, S. J.; Manby, F. R.; Meyer, W.; Mura, M. E.; Nicklass, A.; Palmieri, P.; Pitzer, R.; Rauhut, G.; Schütz, M.; Stoll, H.; Stone, A. J.; and Tarroni, R.; Thorsteinnsson, T.

(29) Douglas, M.; Kroll, N. M. *Ann. Phys. (Leipzig)* **1974**, *82*, 89–155. Hess, B. A. *Phys. Rev.* **1985**, *32A*, 756–763. Hess, B. A. *Phys. Rev.* **1986**, *33A*, 3742–3748.

(30) Watson, J. K. G. *Vibrational Spectra and Structure*; Elsevier: Amsterdam, 1977; Vol. 6.

(31) Pickett, H. M. *J. Mol. Spectrosc.* **1991**, *148*, 371–377.

(32) Nakagawa, T.; Overend, J. *J. Mol. Spectrosc.* **1974**, *50*, 333–348.

(33) Fujitake, M.; Hirota, E. *J. Chem. Phys.* **1989**, *91*, 3426–3430.

(34) Townes, C. H.; Dailey, B. P. *J. Chem. Phys.* **1949**, *17*, 782–796.